https://doi.org/10.70882/yhh1er88

SCIENCE FORUM (JOURNAL OF PURE AND APPLIED SCIENCES) 26, (4) (2026), 1349 - 1365

Science Forum (Journal of Pure and Applied Sciences)

Journal Homepage: https://atbuscienceforum.com.ng/index.php/jpas

Imprints Of Magmatism on Source Rocks of the Yola Arm, Upper Benue Trough: Insights from Biomarker Analysis and Petrography.

Mamidak Miner Iliya[a & c], Timothy Peter Bata[b & c], Solomon Nehemiah Yusuf[c], Raymond Ishaya Daspan[c], Sagir Shuaibu[d]

[a]Department of Geology, Nasarawa State University, Keffi
[b]Department of Geology, Abubakar Tafawa Balewa University, Bauchi State
[c]Department of Geology, University of Jos, Plateau State
[d]Civil and Environment Engineering Department, Air Force Institute of Technology, Kaduna

Abstract

This study assesses the thermal maturity of source rocks affected by magmatism in the Yola Arm of the Upper Benue Trough, Nigeria. The objective was to evaluate the thermal maturity of source rocks exposed around volcanic bodies using biomarker and petrographic analyses and to determine whether magmatic heating produced thermal alterations that overprint normal burial diagenesis. Five outcrop samples representing four stratigraphic intervals associated with volcanic rocks were analyzed using petrographic techniques and Gas Chromatography–Mass Spectrometry (GC–MS). Biomarker-derived thermal maturity parameters, including hopane C_{31} 22S/(22S+22R), sterane C_{29} 20S/(20S+20R), and trisnorhopane Ts/Tm ratios, indicate that the source rocks are thermally mature and generally within early- to peak-oil-window conditions, except for the degraded sample. Petrographic observations further reveal progressive thermal maturation of the organic-rich shales. Progressive darkening, smearing, and partial coalescence of amorphous organic matter (AOM) into discontinuous bitumen-rich lenses constitute textural evidence of kerogen breakdown and bituminization during catagenesis. Spatially localized fabric disruption, bitumen enrichment, and microfracturing observed in some samples provide evidence of short-duration, high-temperature conductive heating events associated with nearby magmatic activity. The combined biomarker and petrographic evidence demonstrate that burial history alone is insufficient to account for the observed variations in source-rock thermal maturity across the Yola Arm. Consequently, the distribution of intrasedimentary magmatic bodies and the spatial extent of their associated thermal aureoles should be incorporated into petroleum-system models to better constrain source-rock maturation patterns and hydrocarbon-generation histories within the basin.

Keywords
Upper Benue,
Thermal Maturity,
Trisnorhopane Thermal Indicator,
Gas Chromatography-Mass Spectrometry,
Biomarker

EISSN: 3156-5190 (Online)
ISSN: 1119-4618 (Print)
JPAS
Faculty of Science, ATBU Bauchi

Corresponding Author: Mamidak Miner Iliya, Department of Geology, Nasarawa State University, Keffi. Email: minermamidak@gmail.com
© 2026 Faculty of Science, ATBU Bauchi. All rights reserved

1.INTRODUCTION

The interaction between magmatism and sedimentary basins is becoming an increasingly important area of research because igneous intrusions and volcanic rocks can profoundly influence the evolution, thermal maturity, and hydrocarbon generation potential of source rocks (Gama et al., 2024; Sun et al., 2020). Through localized heating, magmatic activity within sedimentary successions can alter the temperature regime of basins, affecting porosity, permeability, organic matter maturation, and hydrocarbon preservation. (Sydnes *et al.*, 2019).

These thermal effects may either enhance hydrocarbon generation by accelerating organic maturation or reduce petroleum potential through overmaturation, cracking of hydrocarbons, and destruction of organic matter (Shen et al., 2026; Senger et al., 2017). Consequently, it is essential to understand the influence of magmatism on source rock evolution in order to reduce uncertainty in petroleum system evaluation, particularly in volcanic-influenced sedimentary basins.

Globally, numerous studies have documented the effects of intrusive and extrusive magmatism on organic-rich sedimentary rocks in basins such as the North Atlantic Igneous Province, the Karoo Basin of South Africa, the Neuquén Basin of Argentina, the Vøring and Møre basins of offshore Norway, and the Faroe–Shetland Basin (Scapacan et al., 2018; Aarnes et al.,2015; Aarnes et al., 2011b). These investigations demonstrate that contact metamorphism associated with sills and dykes creates thermal aureoles characterized by elevated vitrinite reflectance, increased Tmax values, changes in biomarker distributions, mineral recrystallization, devolatilization of organic matter, and hydrocarbon generation (Kutovaya et al., 2019).

Biomarker studies have demonstrated that magmatic heating modifies molecular compositions through thermal degradation of hopanes and steranes, isomerization reactions, and preferential destruction of thermally unstable compounds (Peters et al.,2007: Farrimond et al.,1998; Peters et al., 1990), thereby providing valuable indicators of palaeothermal conditions and organic matter evolution.

The effects of magmatism are commonly reflected not only in organic geochemical parameters but also in petrographic characteristics of the affected rocks (Zhang et al., 2026; Li et., al 2024). Petrographic observations provide direct evidence of thermal alteration through recrystallization of clay minerals, development of contact metamorphic fabrics, carbonization of organic matter, microfracturing,and alteration of primary sedimentary textures. The integration of biomarker geochemistry with petrographic analysis therefore highlights the intensity, spatial extent, and geological consequences of magmatic heating on petroleum source rocks.

The Yola Arm of the Upper Benue Trough represents one of the most structurally complex and tectonically active sedimentary basins in Nigeria. The basin formed during the Early Cretaceous as part of the West and Central African Rift System following the separation of the African and South American plates. The evolution of the basin involved multiple phases of extensional tectonics, subsidence, sedimentation, and intermittent magmatic activity associated with the opening of the South Atlantic Ocean (Jia et al.,2025; Adamu et al.,2025).

Thick successions of continental to shallow marine sediments, including organic-rich shale intervals deposited under varying depositional conditions make up the basin. These sediments have long been regarded as having potential for hydrocarbon generation (Didi et al., 2025). However, their petroleum prospectivity is complicated by the widespread occurrence of volcanic rocks, doleritic sills, dykes, and other igneous intrusions emplaced during and after sedimentation.

Previous investigations within the Upper Benue Trough have primarily focused on regional tectonic evolution, stratigraphy, basin architecture, structural framework, and source rock characterization using conventional geochemical techniques. Although several

studies have identified the presence of intrusive and volcanic bodies through field investigations and geophysical data, relatively few have quantitatively assessed their effects on the thermal maturity and molecular composition of adjacent source rocks (Osinowo et al., 2023; Yandoka et al.,2017; Ogunmola et al.,2016; Yandoka et al., 2016). Existing maturity assessments have relied largely on bulk parameters such as Total Organic Carbon (TOC), Rock-Eval pyrolysis, vitrinite reflectance, and Tmax, while the application of biomarker geochemistry integrated with petrographic observations remains limited. Consequently, the mechanisms by which magmatic activity has modified organic matter, altered hydrocarbon generation pathways, and influenced petroleum preservation within the Yola Arm remain insufficiently understood.

Biomarker analysis offers an effective means of reconstructing the thermal and depositional history of source rocks because biomarkers retain information about the origin of organic matter, depositional environment, redox conditions, biodegradation, and thermal evolution. Ratios involving steranes, hopanes, tricyclic terpanes, Ts/Tm, C31 hopane isomerization, moretane/hopane, sterane isomerization, and aromatic maturity parameters provide sensitive indicators of thermal maturity that often respond to localized heating associated with igneous intrusions. When interpreted alongside petrographic evidence such as organic matter texture, mineralogical alteration, contact metamorphic features, and diagenetic overprinting, these molecular signatures enable detailed reconstruction of the thermal imprint of magmatism on source rocks.

In the Yola Arm, where magmatic bodies are spatially associated with sedimentary formations containing potential source rocks, an integrated petrographic and biomarker approach provides an opportunity to distinguish regional burial maturation from localized contact heating. Such integration allows the identification of thermal aureoles, evaluation of the extent of organic matter alteration, and assessment of the implications of magmatic activity for hydrocarbon generation, migration, and preservation. These insights are particularly important for refining petroleum system models in frontier basins where magmatism constitutes a major exploration risk.

This study therefore investigates the imprints of magmatism on source rocks within the Yola Arm of the Upper Benue Trough using integrated biomarker analysis and petrography. Specifically, by characterizing the biomarker composition and maturity of source rocks located at varying distances from igneous bodies, identifying petrographic evidence of thermal alteration and contact metamorphism, and evaluating the influence of magmatic heating on organic matter transformation and hydrocarbon generation potential. The findings contribute to a more comprehensive understanding of volcanic-influenced petroleum systems and provide insights that are applicable to other magmatic sedimentary basins worldwide.

2.GEOLOGICAL SETTING

The Benue trough, also referred to as the Benue rift is a northeastern-trending rift basin that is roughly 800 km long and 120- 150 km wide, and it is filled with approximately 6000m thick of Cretaceous–Palaeogene sediments (Lar et al., 2023).It is a product of the second phase of rifting of the Gondwana supercontinent, which led to the opening of the South Atlantic Ocean, the Gulf of Guinea, and the division of South America from Africa in the Late Jurassic to Early Cretaceous(Adamu et al., 2025; Binks and Fairhead, 1992). It begins at the northernmost point of the Niger Delta Basin. It extends eastward to the Bornu Basin, where it connects to the other intracontinental rift system in Africa, including Sudan, Chad, Niger, and Cameroon. Based on tectonic and geological features, the Trough is divided into lower, middle, and Upper portions (Adamu *et al.*, 2025; Yenne *et al.*, 2025).

The two subdivisions of the Upper Benue Trough are the Gongola and Yola Arms. The Yola arm moves eastward and ends up against the basement rocks of Cameroon, while the Gongola arm moves northward into the Chad Basin (Lar *et al.*,2018; Bessong et al., 2022).

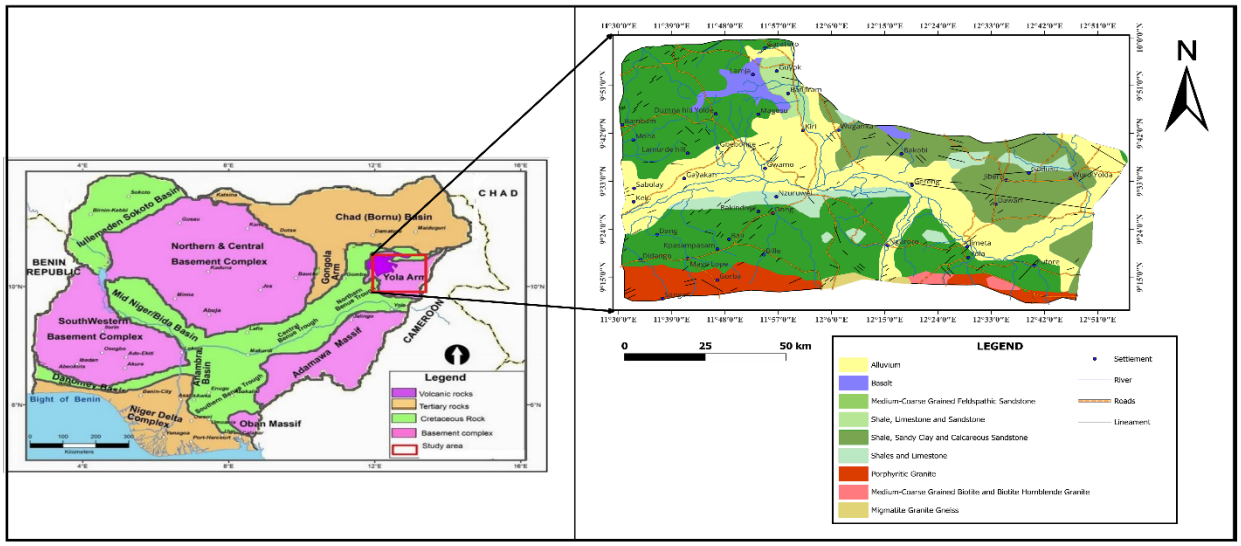


Figure 1: Generalized Geological map of Nigeria showing the location of the study area (Modified after, Yandoka *et al.*, 2020, NGSA, 2004).

In the Yola sub-basin of the Upper Benue Trough, the Bima Formation, the oldest sedimentary lithology in the region, overlies Precambrian Basement rocks unconformably (Didi et al., 2025, Bessong et al,.2022). The Bima Formation is conformably overlain by the transitional/coastal Yolde Formation (Cenomanian), which marks the onset of marine incursion into the Upper Benue Trough (Bata *et al.*, 2015). The significant marine incursion from the upper Cenomanian through the Santonian deposited the Dukul, Jessu, Sekuliye, Numanha, and Lamja Formations within the Yola sub-basin (Lar et al., 2018). Several locations within the Benue Trough experienced tectonic deformation during the mid-Santonian, resulting in folding, faulting, and uplift of Cretaceous sediments deposited before this time (Abubakar et al., 2011). This was followed at the end of the Maastrichtian by a compressive phase (Didi et al., 2024; Zarborski, 2003). Within the Upper Benue Trough, the post-Santonian period marks the end of sedimentation. However, during the Cretaceous, the Yola Arm hosted significant volcanic intrusions emplaced during tectono-magmatic episodes, most of which are spatially associated with regional fault zones (Benkhelil, 1989). Benkhelil (1989) also reported that Tertiary volcanic activity in Nigeria was intense in the Upper Benue Trough, where extensive lava flow formed the Biu and Longuda Plateau.

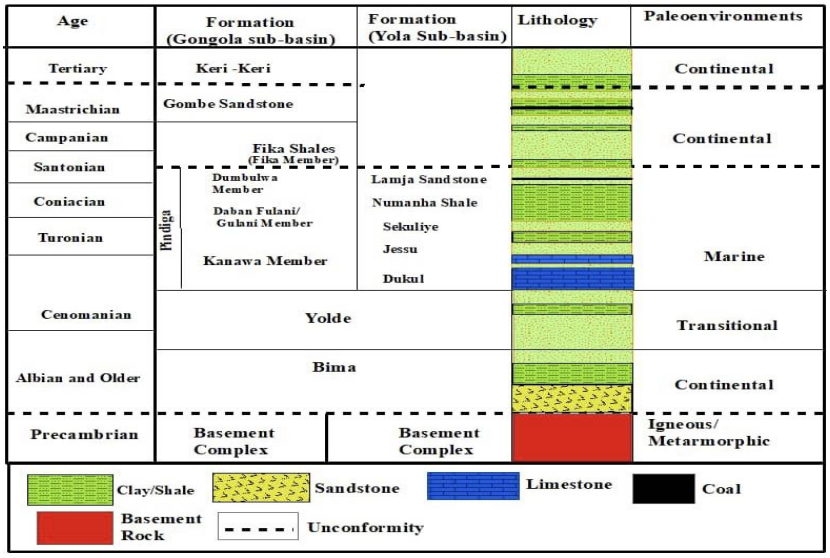


Figure 2: Stratigraphic sequence of the Northern Benue Trough, Nigeria (After, Abubakar *et. al.*, 2008).

2.METHODOLOGY

Five outcrop samples of the source were analyzed. The samples analyzed are representative of the entire population of samples collected during the fieldwork, taking into account proximity to the volcanics and Tmax values. The samples represent organic-rich intervals of the Dukul, Numanhan, and Sekuliye formations. Thin sections of these samples were prepared using standard procedures. Optical microscopy under transmitted light was used to evaluate mineralogical composition, textural relationships, fabric development, and the state of organic matter preservation and thermal modification.

Saturate fractions from the source rocks extracted using a standard procedure involving an organic solvent (DCM) and a hexane-dichloromethane mixture (97:3 v/v). The oil-organic solvent mixture was placed in a rotary evaporator, which separated the oil into maltenes and asphaltenes. Thin-layer chromatography was then employed to divide the extracted maltene component into polar, aromatic, and saturated fractions. Gas chromatography-mass spectrometry (GC–MS) was then used to investigate the saturated fraction in the University of Aberdeen's Geochemistry Lab in the United Kingdom. An Agilent 6890N GC with a 50-m-long J & W DB-5 column connected to a 5975 MSD and a quadrupole mass spectrometer operating in selected-ion monitoring (SIM) mode at an ionization energy of 70 eV was used to perform the GC-MS study. The samples were manually injected into a split/splitless injector operating in splitless mode for 2 minutes at a purging rate of 40 mL/min (e.g., Bata *et al.*, 2024). The general circulation oven temperature range was 80 to 295°C. Chemicals in the investigated oil residues were identified by comparing their retention times with those of well-characterized reference samples.

To obtain quantitative biomarker data for each sample, the response times of isoprenoids, steranes, diasteranes, and hopanes were assessed in Total Ion Count (TIC) mass chromatograms at m/z 85, 217, and 191. Thermal maturities of oils were calculated from the Ts/Tm terpanes and the 20S/(20S + 20R) ratio for normal steranes, based on the increasing fraction of the S isomer with maturity (Elfadly *et al.*, 2017; Peters and Moldowan, 1993). In essence, the top of the oil window is reached when these maturity indicators reach equilibrium.

A summary of biomarker data and other calculated ratios for the studied petroleum source rocks, collected from different locations near areas intruded by volcanics, is presented in Table 1. Total ion current (TIC) and single ion monitoring (SIM) modes were used to record the distributions of normal alkanes, isoprenoids, terpanes, and steranes. The TIC and SIM mass chromatograms (m/z 85, 191, and 217) were used as references for the detailed biomarker characteristics investigated in this study. Fragmentograms for peaks were identified based on retention time and previous work or literature.

Isoprenoids and n-alkanes in the extracted source rock samples were identified using a total ion chromatogram and m/z 85. Figure 3(a-d) shows the TIC fragmentogram for the studied samples. Compounds present in the extracts include n-alkanes, mid-methyl alkanes, and isoprenoids in the form of pristane (Pr) and phytane (Ph) (see Figure 3(a-d)). Calculated values are presented in Tables 1 and 2. Pristane/phytane (Pr/Ph) ratios range from 0.47 to 3.78 (average: 1.85).

3. RESULTS

3.1 Biomarker Analysis

Table 1; Summary of biomarker data and other calculated ratios for the studied petroleum source rocks

Sample	Dist. (m)	TOC (wt.%)	HI	Tmax (°C)	Isoprenoid ratios				Maturity biomarker ratios				Sterane distribution		
					Pr/Ph	Pr/nC$_{17}$	Ph/nC$_{18}$	Ts/Tm	C32 22S/(22S+22R)	C27 20S/(20S+20R)	C28 20S/(20S+20R)	C29 20S/(20S+20R)	C27 (%)	C28 (%)	C29 (%)
DFM 4	15	2.11	56	451	0.47	0.45	1.83	1.90	0.54	0.54	0.47	0.52	25.87	33	40.73
DFM 5	30	1.49	56	442	0.90	0.72	0.80	1.23	0.54	0.50	0.50	0.49	25.58	33	41.42
NFM 20	45	2.31	62	443	1.46	0.95	0.65	1.25	0.52	0.49	0.50	0.47	43.16	32	24.38
SFM 12	—	1.30	57	441	2.63	2.33	0.94	1.09	0.52	0.47	0.50	0.42	41.27	31	26.98
SFM 13	15	—	62	446	3.78	0.96	0.90	—	—	0.36	0.66	0.45	55.30	36	8.17

Note: Dist. = proximity to intrusion; TOC = total organic carbon; HI = hydrogen index. C32 22S/(22S+22R) denotes homohopane isomerization; C27–C29 20S/(20S+20R) denote sterane isomerization ratios.

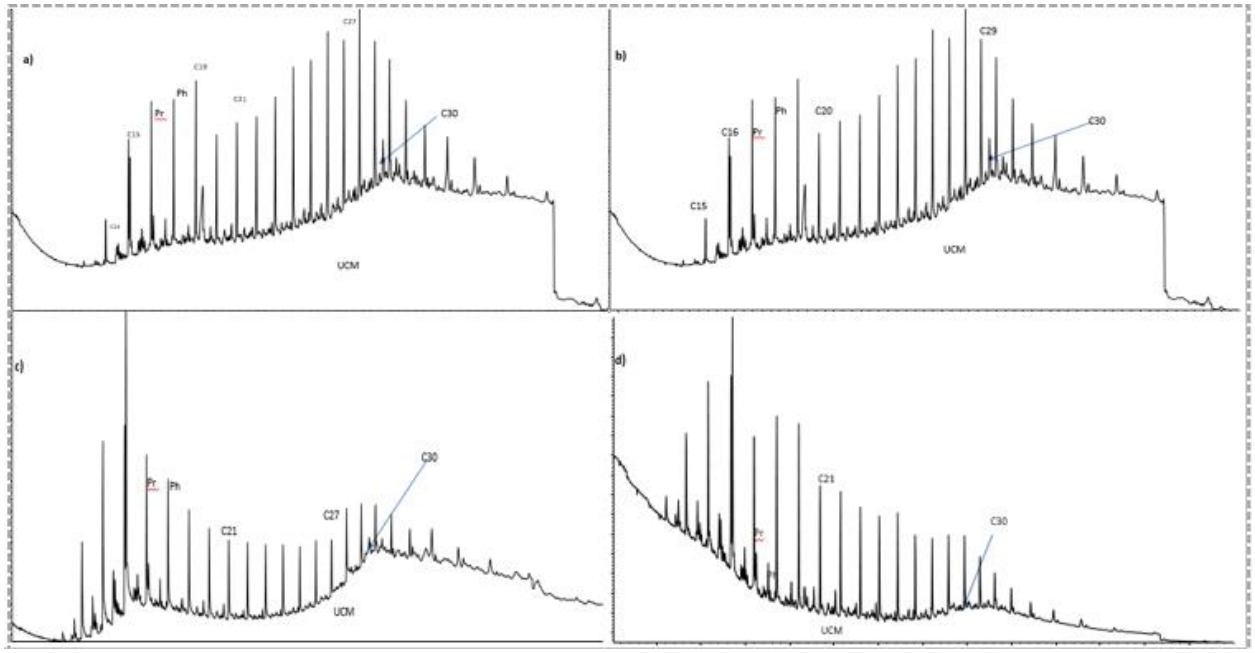


Figure 3(a-d) Total ion current (TIC) fragmentogram of the saturate fraction for the studied source rocks picked in the vicinity of volcanics. Note unresolved complex mixture (UCM) "humps" in a, b, and c consistent with oils that have undergone biodegradation.

Steranes in the extracted source rocks were identified at m/z 217, as shown in Figure 4(a-d). The quantities of steranes were determined from the isomer distribution in the m/z 217 fragmentogram of the analyzed source rocks. The distribution of regular steranes and other sterane-derived parameters is presented in Table 2. The relative abundances of the regular sterane compounds (%C27, %C28, and %C29) indicate that C29 aaa 20R sterane is most abundant in the extracted source rock samples DFM 4 and DFM 5. In contrast, C28 aaa 20R sterane is abundant in samples NFM 20, SFM 12, and SFM 13. C29 aaa 20R sterane ranges from 25.28–55.30% (average: 29.81%), C28 aaa 20R sterane from 31.75–36.52% (average: 53.37%), and C27 aaa 20R sterane from 8.17% to 41.42% (average: 19.60%). Sterane fingerprint parameters such as C2920S/(20S + 20R), C2820S/(20S + 20R), and C2720S/(20S + 20R) from m/z 217 fragmentogram peaks were calculated. Source rocks of the Dukul Formation (DFM 4 and DFM 5) from Bambam, picked closest to and at the midpoint of the volcanic intrusions, have sterane maturity parameters aaa C2720S/(20S+20R), aaa C2820S/(20S+20R), and aaa C2920S/(20S+20R) with values of 0.54, 0.47, 0.52, and 0.50, 0.50, 0.49, respectively. Likewise, the analyzed sample from the Numanhan Formation has values of 0.49, 0.50, and 0.47. The analyzed samples from the Sekuliye Formation have values of 0.47, 0.50, and 0.42 for the second sample and 0.36, 0.36,0.66, and 0.45, respectively.

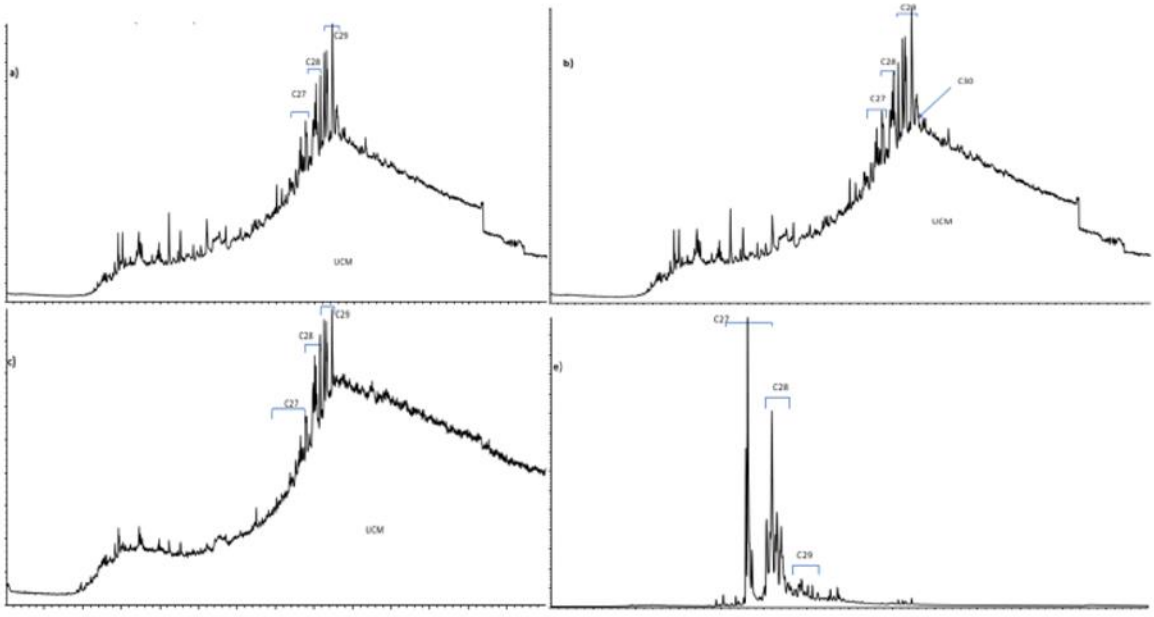


Figure 4(a-d): m/z 217 fragmentogram of the saturate fraction for the studied source rock picked in the vicinity of volcanics. Note unresolved complex mixture (UCM) "humps" in a, b, and c consistent with oils that have undergone biodegradation.

Tricyclic terpanes (TT) ranging from C19 to C29, along with hopanes and homohopanes, were identified at m/z 191. Figure 5(a-d) presents the m/z 191 fragmentogram for the saturate fraction of the source rocks within the study area. The m/z 191 fragmentogram reveals well-preserved terpanes, tricyclic terpanes (C19–C30), and pentacyclic triterpenes, including Ts, Tm, norhopanes, and regular hopanes (C27–C35). Gamacerene is detected in all rock extracts, except in sample SFM 13, which has been completely thermally cracked.

The two source rock samples from the Dukul formation have Ts/Tm ratios of 1.9 and 1.23, respectively, and a homohopane isomerization ratio of 0.54 for

C3222S/(22R+22S). The hopane characteristics of the source rock from the Numanhan Formation as shown in the m/z 191 fragmentogram in Figure 5(a-d), have a Ts/Tm ratio of 1.25 and a homohopane isomerization ratio of 0.57 for C3222S/(22R+22S). By contrast, the source rock sample from the Sekuliye Formation under study has a Ts/Tm ratio of 0.62 and a homohopane isomerization ratio of 0.57 for C3222S/(22R+22S).

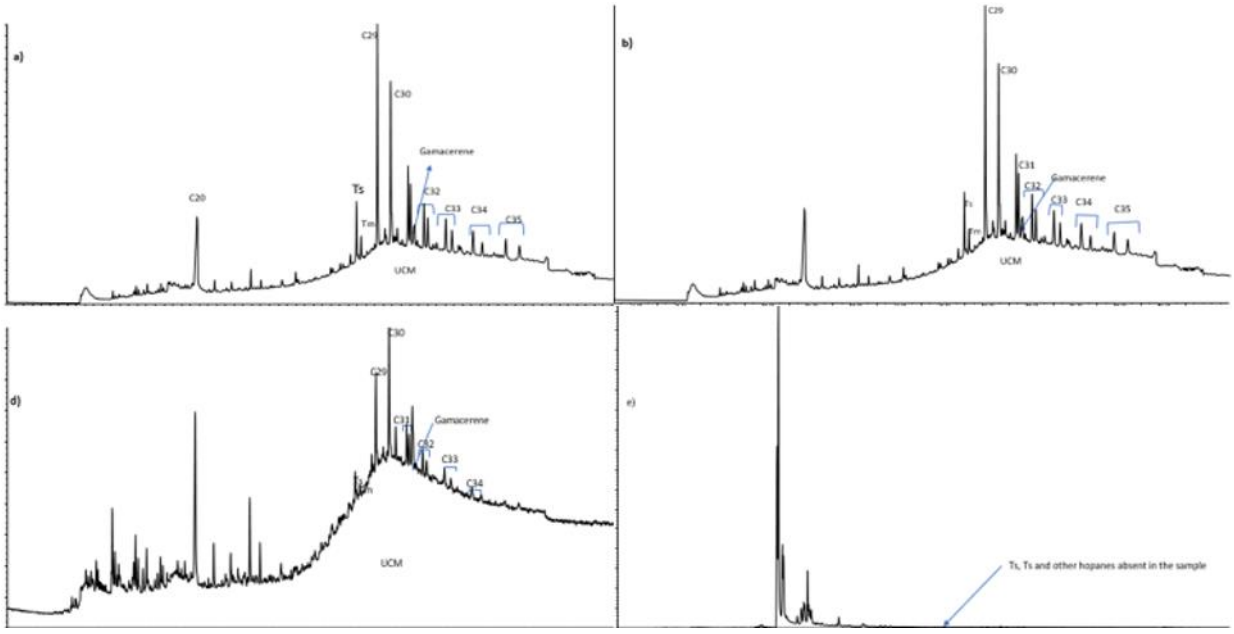


Figure 5 (a-d): M/z 191 fragmentogram of the saturate fraction for the studied source rocks picked in the vicinity of volcanics.

Trisnorhopane ratios are key biomarker parameters in organic geochemistry for assessing thermal maturity in sedimentary rocks and oils. These ratios track differences in isomerization and stability among specific C27 trisnorhopane compounds during catagenesis.

The primary trisnorhopane ratio is Ts/Tm, where Ts denotes 18a(H)-22,29,30-trisnorneohopane and Tm denotes 17a(H)-22,29,30-trisnorhopane. This ratio increases with thermal maturity, typically from values below 0.2 in immature samples to over 0.5–0.6 in mature samples entering the oil window, due to the greater thermal stability of Ts relative to Tm. These ratios complement sterane and hopane isomerization parameters but can vary with source depositional environment or facies (Zhang et al., 2002). Ts/Tm ratios for the samples were calculated (Table 1), and the trisnorhopane thermal indicator (Ts: Tm) for each source rock analyzed, except for the sample from the Sekuliye formation, which had missing Ts and Tm peaks due to complete cracking from thermal alteration, is shown in Figure 6. The chart also shows the equivalent vitrinite reflectance for each sample (Machel et al., 1995). The trisnorhopane thermal indicator (Ts: Tm) for the extracts from the source rocks varied between 1.09 and 1.9.

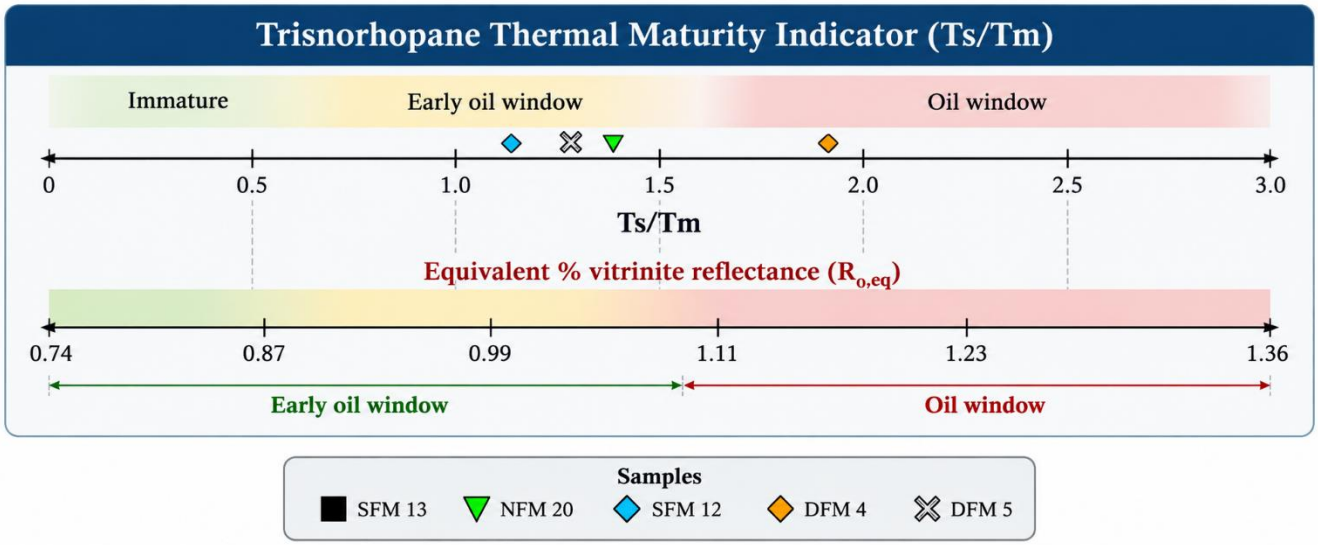


Figure 6: Trisnorhopane thermal indicator (Ts: Tm ratio) showing thermal maturity levels comparable with oils generated within the oil window.

Figure 7 also shows a cross-plot of steranes versus hopanes. Other biomarker maturity parameters, including the ratios of C32 22S/(22S + 22R) homohopanes and C29 sterane 20S/(20S + 20R) (Tables 1 and 2), are also used. The C32 22S/(22S + 22R) homohopane ratio and the dominance of S-isomers over R-isomers in the homohopane series (C31—C35) (Fig. 6a-d) also indicate that the source rocks are in the immature to mature stages of hydrocarbon generation. In addition, the C29 20S/(20S + 20R) sterane ratio is directly proportional to thermal maturity; it increases with increasing maturity. The C29 20S/(20S + 20R) value (Table 2) indicates that the source rocks are in the oil generation window (Peters and Moldowan 1993; Peters et al., 2005).

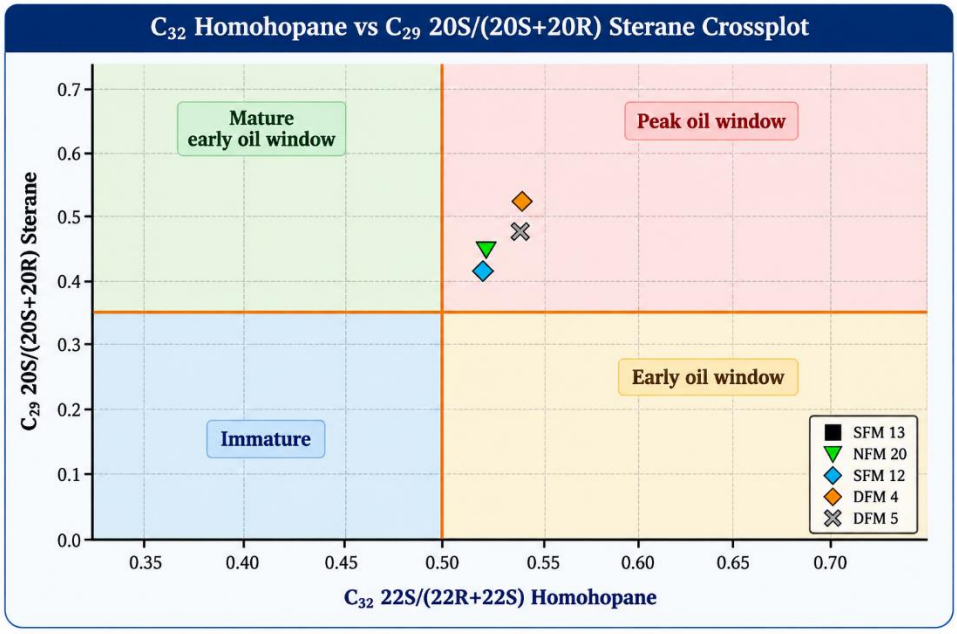


Figure 7: Cross plot of steranes vs hopanes; all the studied source rock samples have thermal maturity levels comparable with oils generated within the oil window.

3.2 Petrography

Clear petrographic heterogeneity is observed among the samples (Figure 8(a) and (b), figure 9 (a) and (b), Figure10 (a) and (b), and Figure4(a) and (b)). Some of the samples retain well-preserved lamination, continuous clay alignment, and minimally altered organic matter. In certain samples signs of localized disruption of laminae, enhanced compaction textures, and evidence of thermal alteration of organic constituents were evident. Other samples exhibited, organic matter textural modification, including darkening, local coalescence, and partial smearing along laminae.

These progressive modifications suggest conductive heating effects associated with nearby volcanic bodies rather than uniform regional burial metamorphism. Importantly, despite evidence of thermal overprinting, most samples do not exhibit pervasive recrystallization or hornfelsic textures, indicating that alteration generally remained within sub-metamorphic conditions.

These features are interpreted as the petrographic expression of thermal maturation and incipient bituminization associated with elevated heat flow. The spatial variability in organic matter texture and optical properties therefore reflects a gradient in thermal overprinting related to proximity to magmatic intrusions

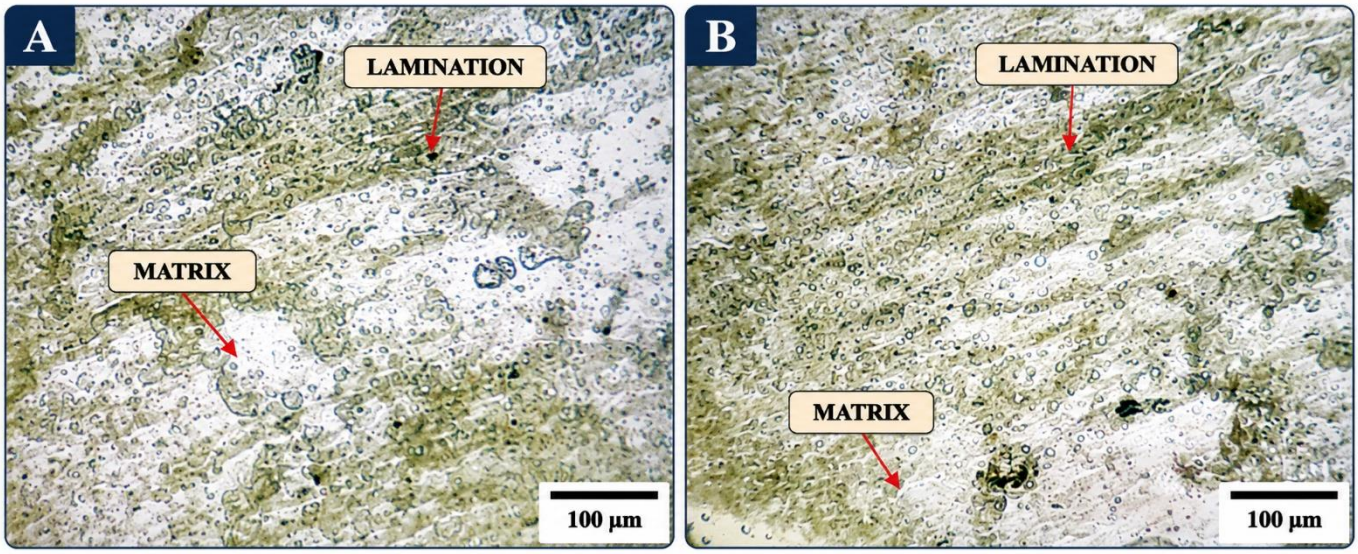


Figure 8 (A) and (B): Photomicrograph showing different views of shales of the Dukul Formation, which are finely laminated, clay-rich, showing parallel alignment of platy clay minerals and disseminated amorphous organic matter preserved along bedding planes. Fabric preservation indicates low-grade thermal overprint.

The shale matrix is predominantly grey to greenish and is composed chiefly of illite and illite–smectite (I/S) mixed-layer clay minerals (Plates 8a,b; 9a,b). The greenish-grey coloration is consistent with progressive burial diagenesis and clay mineral transformation within a reducing depositional environment. The dominance of illitic phases suggests advanced diagenetic modification, while the persistence of mixed-layer I/S indicates incomplete ordering, compatible with sub-metamorphic thermal conditions. No pervasive recrystallization of mica, development of spotted textures, or formation of hornfelsic fabric is observed in the majority of samples, implying that peak temperatures did not generally reach contact-metamorphic conditions. An exception is the sample from Nuhaman formation (Figure10 a and b), which displays a distinctly contact-baked character. Here, the shale exhibits textural homogenization and recrystallization consistent with localized high-temperature alteration in close proximity to magmatic bodies.

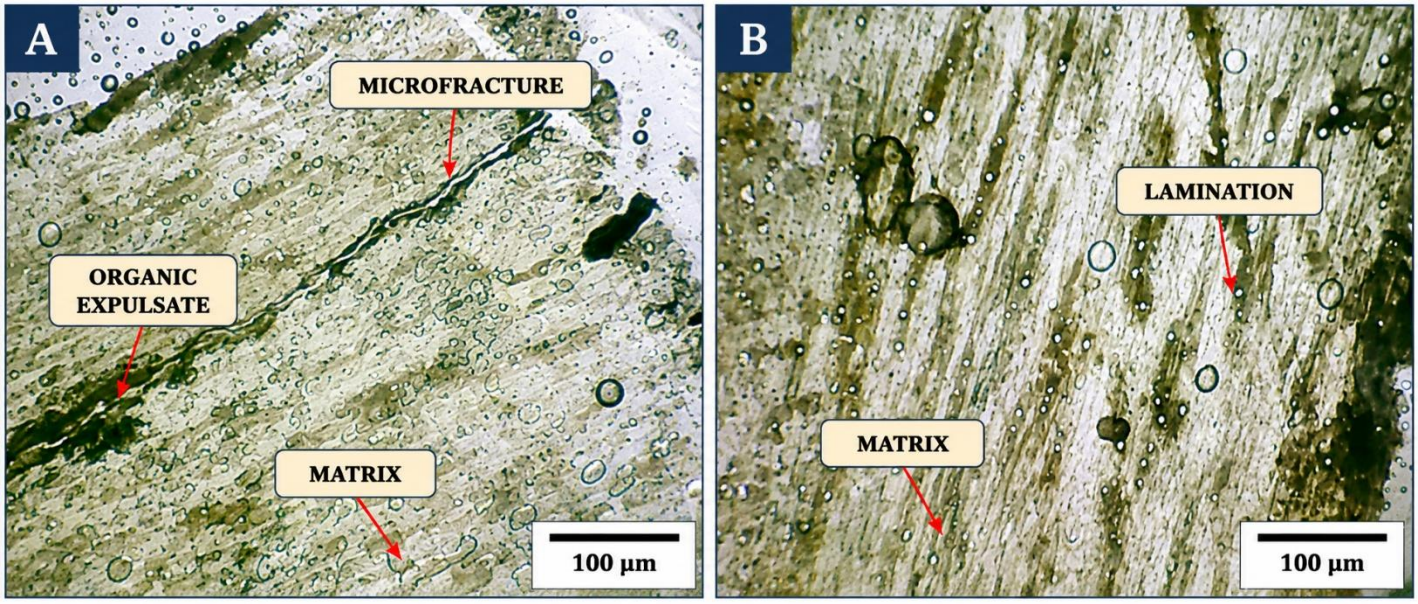


Figure 9: Photomicrographs showing (A): Laminated shales of the Dukul Formation with dark, bedding-parallel organic streaks and greenish-grey clay matrix, interpreted as thermally altered organic matter and smectite –illite transformation. (B) Shales from the Sekuliye Formation exhibiting a transition from well-laminated fabric into a dark, massive, bitumen-rich zone with localized disruption of lamination, interpreted as proximity to a magmatic heat source.

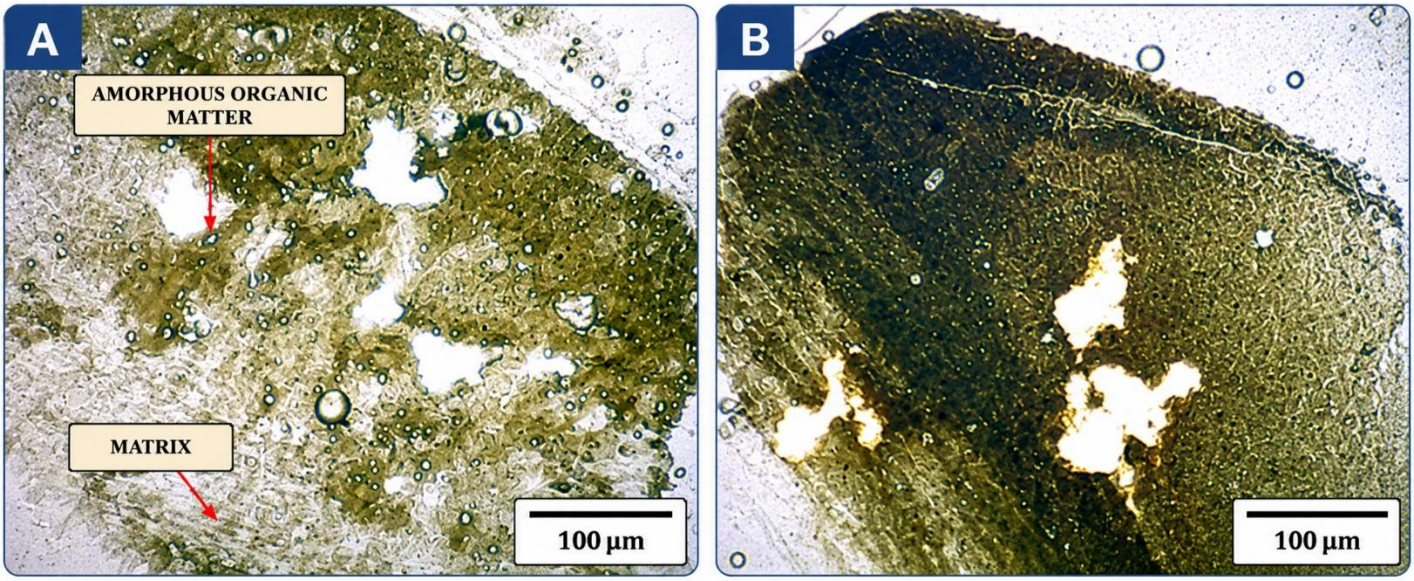


Figure 10: Photomicrograph of (A)Shales of the Numanhan Formation exhibiting smeared, amorphous organic matter lenses indicating in-situ kerogen cracking and short-distance bitumen migration during heating. (B) contact-baked shale of the Numanhan showing a massive, recrystallized fabric with complete loss of primary lamination, indicative of intense thermal alteration. Note: The Bright patches are due to the preparation of the sample.

Organic matter is present predominantly as amorphous, dark streaks and diffuse patches aligned parallel to bedding planes (figure 10a). The bedding-concordant distribution reflects primary depositional control and compactional flattening. The absence of structured terrestrial phytoclasts suggests a dominantly amorphous organic assemblage, likely marine-derived, consistent with oil-prone kerogen types. The organic matter exhibits progressive optical darkening, smearing, and local coalescence into discontinuous bitumen-rich lenses, particularly in zones where lamination is partially disrupted (figure 10b). These textures are interpreted as the petrographic expression of thermal maturation and bituminization. The migration and concentration of organic material into lenses indicate mobilization during heating, with redistribution along planes of mechanical weakness such as bedding surfaces and microfractures.

Localized zones of fabric modification are observed where well-preserved laminated shale grades laterally or vertically into dark, massive intervals enriched in organic matter (Plate 9b). These transition zones show partial destruction of lamination, increased optical density of the matrix, and concentration of amorphous organic material.

Subtle microfractures and linear dark seams occur along laminae and at the boundaries between altered and unaltered domains. These features likely represent thermally induced contraction fractures or overpressure-related microfracturing associated with hydrocarbon generation and expulsion (figure 9a). Their preferential development along bedding underscores the mechanical anisotropy imposed by early compactional fabric.

In contrast to the laminated and partially modified shales,the examined source rock of the Nuhaman formation displays a massive, dark groundmass characterized by complete obliteration of primary lamination and development of a recrystallized microcrystalline texture (figure10 a and b). The absence of recognizable clay alignment and preserved organic matter streaks indicates intense thermal alteration. This texture is consistent with contact metamorphism approaching incipient hornfels conditions, where elevated temperatures have driven mineral recrystallization and organic matter destruction. The loss of primary sedimentary structures and homogenization of the matrix signify thermal conditions exceeding the typical oil window, potentially resulting in overmaturation and pyrobitumen formation.

Collectively, the shale fabrics range from well-preserved laminated textures with intact compactional clay alignment to completely recrystallized, massive fabrics lacking primary sedimentary structures. This continuum reflects a progressive thermal overprinting spectrum, extending from background burial diagenesis to intense, localized heating adjacent to magmatic intrusions. The predominance of illite and illite–smectite mixed-layer clays, coupled with preservation of lamination in most samples, constrains regional alteration to advanced diagenetic but sub-metamorphic conditions. However, the presence of contact-baked textures and recrystallized fabrics in proximal samples demonstrates that localized conductive heating significantly modified mineralogy, microstructure, and organic matter distribution (figure 10). Thus, the petrographic data provide compelling microtextural evidence for spatially heterogeneous thermal evolution, controlled by both burial history and proximity to volcanic heat sources.

4. DISCUSSION

The integrated petrographic and biomarker analysis approach demonstrate that the thermal evolution and hydrocarbon potential of the Cretaceous organic-rich shales in the Yola Arm, Upper Benue Trough, were controlled by the combined influence of depositional conditions, burial diagenesis, and localized magmatic heating. Rather than representing a simple burial-driven maturation history, the source rocks record a complex thermal evolution in which intrasedimentary magmatism imposed significant spatial heterogeneity on organic matter preservation, maturation pathways, and hydrocarbon generation efficiency.

4.1. Depositional Controls on Organic Matter Preservation

The petrographic and biomarker data indicate that the Cretaceous organic-rich shales of the Yola Arm were deposited under conditions favorable for organic matter preservation and subsequent hydrocarbon generation. Fine-grained lithofacies, well-preserved parallel lamination, and abundant amorphous organic matter (AOM) indicate sedimentation in low-energy, restricted marine environments under dysoxic to suboxic bottom-water conditions, where limited bioturbation and reduced oxidation promoted the preservation of labile organic matter (Tissot & Welte, 1984). The predominance of AOM over terrestrial phytoclasts suggests a predominantly marine algal source with subordinate terrestrial input, corresponding to Type II to mixed Type II/III kerogen with good oil-generative potential (Peters & Cassa, 1994).

Biomarker signatures support this depositional interpretation. Pristane/phytane (Pr/Ph) ratios, generally between 1 and 3, together with sterane distributions dominated by C29 but containing significant C27 homologues, indicate mixed marine and terrestrial organic matter deposited under predominantly suboxic to oxic conditions (Volkman 2005; Sendjaja et al., 2024). The agreement between petrographic observations and biomarker characteristics demonstrates that the Yola Arm source rocks accumulated under environmental conditions conducive to both high primary productivity and efficient preservation of organic matter, providing the foundation for effective petroleum source rock development.

4.2. Magmatic Controls on Thermal Maturation and Hydrocarbon Generation

Although burial diagenesis initiated organic matter maturation, the integrated petrographic, and biomarker evidence demonstrates that localized magmatic heating exerted the dominant control on thermal evolution across the study area. Progressive darkening and coalescence of AOM into bitumen-rich lenses, together with illite–smectite transformation, indicate increasing thermal maturity during catagenesis (Horsfield & Rullkötter, 1994; Hower et al., 1976). However, the localized occurrence of recrystallization, disrupted lamination, microfracturing, and destruction of organic matter in samples proximal to intrusions indicates conductive heating associated with contact aureoles rather than burial alone (Svensen et al., 2004; Aarnes et al., 2010).

Biomarker maturity parameters independently corroborate these observations. Low Pr/n-C17 and Ph/n-C18 ratios, Ts/Tm values between approximately 1.09 and 1.90, sterane isomerization ratios, and equivalent vitrinite reflectance values of 1.0–1.17% Ro collectively indicate that most samples attained late oil-window maturity, consistent with previous studies from the Yola Arm (Yandoka et al., 2016, 2017). In contrast, progressive depletion of steranes and diminished m/z 217 sterane peaks in samples nearest the intrusions indicate localized thermal cracking and overmaturation. The most altered sample records contact metamorphism approaching incipient hornfels conditions, where primary sedimentary fabrics and recognizable organic matter have been largely obliterated, suggesting exhaustion of oil-generating potential and possible secondary thermogenic gas generation.

4.3. Implications for the Petroleum System of the Yola Arm

The integrated approach demonstrates that the petroleum system of the Yola Arm evolved under a dual thermal regime comprising regional burial diagenesis superimposed by localized magmatic heating. This interaction produced significant spatial variability in source-rock maturity, hydrocarbon generation, and expulsion efficiency. Source rocks located distal to intrusive bodies generally remained within the optimal oil window, whereas those adjacent to intrusions experienced accelerated maturation, localized overmaturation, and, in extreme cases, thermal destruction of organic matter.

Magmatism therefore exerted both constructive and destructive influences on petroleum prospectivity.

Elevated heat flow promoted rapid kerogen conversion and enhanced hydrocarbon generation, while thermally induced microfracturing likely improved primary hydrocarbon expulsion through transient increases in permeability. Conversely, intense contact metamorphism locally degraded source-rock quality by converting kerogen to pyrobitumen and destroying primary porosity. Simultaneously, temperature-driven clay mineral transformations may have modified seal integrity and influenced fluid migration pathways through changes in shale fabric and capillary properties (Bjørlykke & Jahren, 2012).

These findings demonstrate that burial history alone is insufficient to explain maturity variations within the Yola Arm. Instead, the distribution of intrasedimentary magmatic bodies and their associated thermal aureoles must be incorporated into petroleum system models. The integration of petrographic and biomarker evidence therefore provides a robust framework for predicting maturity distribution and identifying prospective hydrocarbon kitchens in volcanic-influenced sedimentary basins of the Upper Benue Trough.

5. CONCLUSIONS

This study evaluates the thermal maturity and alteration of source rocks around volcanics using biomarker and petrographic analyses to determine characteristics that overprints normal burial diagenesis in the Upper Benue Trough Nigeria. Specifically, this study demonstrates the following:

- From the Trisnorhopane thermal indicators (Ts:Tm ratio) of the studied source rocks, as well as their C3222S/(22R+22S) homohopane isomerization ratios, their thermal maturity levels are comparable to those within the peak of oil window except for the degraded sample.
- Greenish-grey matrix and well-developed clay fabric are interpreted as reflecting progressive illite–smectite transformation.
- Progressive thermal maturation of the organic-rich shales is exhibited by progressive darkening, smearing, and partial coalescence of AOM into discontinuous bitumen-rich lenses represent textural manifestations of kerogen breakdown and bituminization during catagenesis. These features are characteristic of early- to peak-oil-window conditions.
- Spatially localized fabric disruption, bitumen enrichment, and microfracturing within some of the samples is indicative of short-duration, high-temperature conductive heating events rather than prolonged regional burial metamorphism.

These findings demonstrate that burial history alone is insufficient to explain maturity variations within the Yola Arm. Instead, the distribution of intrasedimentary magmatic bodies and their associated thermal aureoles must be incorporated into petroleum system models.

REFERENCES

Aarnes, I., Planke, S., Svensen, H., Corfu, F. (2010). Contact metamorphic devolatilization of shales in the Karoo Basin, South Africa: Implications for the Permian–Triassic boundary environmental crisis. *Earth and Planetary Science Letters*, 295(1-2), 123-132.

Aarnes, I., Svensen, H., Polteau, S., & Planke, S. (2011). Contact metamorphic devolatilization of shales in the Karoo Basin, South Africa, and the effects of multiple sill intrusions. *Chemical Geology*, *281*(3-4), 181-194.

Aarnes, I., Planke, S., Trulsvik, M., & Svensen, H. (2015). Contact metamorphism and thermogenic gas generation in the Vøring and Møre basins, offshore Norway, during the Paleocene–Eocene thermal maximum. *Journal of the Geological Society*, *172*(5), 588-598.

Abubakar, M. A. M. (2011). Evaluation of the Petroleum Potentials of the Northeastern Nigerian Sedimentary Basins: Northeastern Nigerian Sedimentary Basins. *Journal of Energy Policy Research and Development (JEPRD)*, *1*(1), 25-56.

Adamu, L. M., Obaje, N. G., Adeoye, A. J., & Oladimeji, R. G. (2025). Litho-structural–depth interpretation of high-resolution aeromagnetic, radiometric, and field data over Akiri area, Central Benue Trough, Nigeria: implications for hydrocarbon prospectivity. *Arabian Journal of Geosciences*, *18*(8), 152.

Bata, T., Parnell, J., Samaila, N. K., Abubakar, M. B., Maigari, A. S. (2015). Geochemical evidence for a Cretaceous oil sand (Bima oil sand) in the Chad Basin, Nigeria. Journal ofAfrican Earth Sciences, 111, 148-155.

Bata, T., Awadh, S., Al-Mimar, H., Yusuf, S., Elijah, E., Lawan, A., & Wakili, W. (2024). Unveiling the Mysteries of Fractured Basement Oil Residues in the Upper Benue Trough, Nigeria. *The Iraqi Geological Journal*, 205-220.

Benkhelil, J. (1989). The origin and evolution of the Cretaceous Benue Trough (Nigeria). *Journal of African Earth Sciences (and the Middle East)*, *8*(2-4), 251-282.

Bessong, M., Bomolomo, M. V., Mbesse, C. O., Mbassa, B. J., Mioumndé, A. P., Hell, J. V., ... & Samankassou, E. (2022). The Garoua Formation of the Upper Benue Trough (Cameroon), as a potential lateral extension of the Bima Formation (Nigeria): evidence from geomorphology, facies analysis, petrology and geochemistry. *Arabian Journal of Geosciences*, *15*(9), 915.

Binks, R. M., & Fairhead, J. D. (1992). A plate tectonic setting for Mesozoic rifts of West and Central Africa. *Tectonophysics*, *213*(1-2), 141-151.

Bjørlykke, K., Jahren, J. (2012). *Petroleum Geoscience: From Sedimentary Environments to Rock Physics*. Springer.

Didi, C. N., Osinowo, O. O., Akpunonu, O. E., & Nwali, O. I. (2024). Petroleum system and hydrocarbon potential of the Kolmani Basin, Northeast Nigeria: *Journal of Sedimentary Environments*, *9*(1), 145-171.

Didi, C. N., Osinowo, O. O., Akpunonu, O. E., & Okeke, S. E. (2025). Multi-disciplinary approach to evaluate hydrocarbon potential in the Bornu Basin, Northeastern Nigeria. *Journal of African Earth Sciences*, *230*, 105742.

Elfadly, A. A., Ahmed, O. E., & El Nady, M. M. (2017). Assessment of organic content in surface sediments of the Suez Gulf, Egypt, using biological marker indicators of normal alkanes, terpanes, and steranes. *Egyptian journal of petroleum*, *26*(4), 969-979.

Farrimond, P., Taylor, A., & TelnÆs, N. (1998). Biomarker maturity parameters: the role of generation and thermal degradation. *Organic Geochemistry*, *29*(5-7), 1181-1197.

Gama, J. W., Kiswaka, E. B., & Mshiu, E. E. (2025). Influence of igneous intrusions on maturation of the Cretaceous-Eocene source rocks of the offshore Tanzanian Basin. *Acta Geochimica*, *44*(2), 387-403.

Horsfield, B., Rullkötter, J. (1994). Geochemistry of petroleum generation and migration. In: Magoon, L.B., Dow, W.G. (eds) *The Petroleum System—From Source to Trap*. AAPG Memoir, vol 60, pp 213-231.

Hower, J., Eslinger, E.V., Hower, M.E., Perry, E.A. (1976). Mechanism of burial metamorphism of argillaceous sediment: 1. Mineralogical and chemical evidence. *Geological Society of America Bulletin*, 87(5), 725-737.

Jia, Y., Suhail, H. A., Zhou, G., Hou, Y., Tian, J., Liu, D., & Yin, L. (2025). Impact of Inversion Tectonics on Hydrocarbon Trapping in Delo Depression, Bongor Basin, Southwestern Chad. In *Doklady Earth Sciences* (Vol. 522, No. 1, p. 6). Moscow: Pleiades Publishing.

Kutovaya, A., Kroeger, K. F., Seebeck, H., Back, S., & Littke, R. (2019). Thermal effects of magmatism on surrounding sediments and petroleum systems in the northern offshore Taranaki Basin, New Zealand. *Geosciences*, *9*(7), 288.

Lar, U. A., Bata, T. P., Dibal, H. U., Daspan, R. I., Isah, L. C., Fube, A. A., & Bassi, D. A. (2018). Field, petrographic and geochemical studies of basement, clastic and carbonate petroleum reservoirs in the Northern Benue Trough, Nigeria. *Pet Technol Dev J*, *8*(2), 36-52.

Lar, U. A., Bata, T., Dibal, H., Yusuf, S. N., Lekmang, I., Goyit, M., & Yenne, E. (2023). Potential petroleum prospects in the middle Benue trough, central Nigeria: Inferences from integrated applications of geological, geophysical and geochemical studies. *Scientific African*, *19*, e01436.

Lar, U. A., Bata, T., Dibal, H., Yusuf, S. N., Lekmang, I., Goyit, M., & Yenne, E. (2023). Potential petroleum prospects in the middle Benue trough, central Nigeria: Inferences from integrated applications of geological, geophysical and geochemical studies. *Scientific African*, *19*, e01436.

Li, C., Zeng, J., Wang, M., Long, H., & Liu, S. (2024). Influence of magmatic intrusion on abnormal hydrocarbon generation and expulsion of source rock: A case study of the Dongying Sag, Bohai Bay Basin. *Acta Geologica Sinica-English Edition*, *98*(5), 1322-1337.

Machel, H. G., Krouse, H. R., & Sassen, R. (1995). Products and distinguishing criteria of bacterial and thermochemical sulfate reduction. *Applied geochemistry*, *10*(4), 373-389.

Ogunmola, J. K., Ayolabi, E. A., & Olobaniyi, S. B. (2016). Structural-depth analysis of the Yola Arm of the Upper Benue Trough of Nigeria using high resolution aeromagnetic data. *Journal of African Earth Sciences*, *124*, 32-43.

Osinowo, O. O., Abdulmumin, Y., & Faweya, T. V. (2023). Analysis of high-resolution airborne-magnetic data for hydrocarbon generation and preservation potential evaluation of Yola sub-basins, northern Benue Trough, northeastern Nigeria. *Energy Geoscience*, *4*(1), 33-41.

Peters, K.E., Moldowan, J.M. (1993). The Biomarker Guide: Interpreting Molecular Fossils in Petroleum and Ancient Sediments. Prentice Hall, Englewood Cliffs, NJ.

Peters, K. E., Moldowan, J. M., & Sundararaman, P. (1990). Effects of hydrous pyrolysis on biomarker thermal maturity parameters: Monterey phosphatic and siliceous members. *Organic geochemistry*, *15*(3), 249-265.

Peters, K.E., Cassa, M.R. (1994). Applied Source Rock Geochemistry. In: Magoon, L.B., Dow, W.G. (eds) *The Petroleum System—From Source to Trap*. AAPG Memoir, vol 60, pp 93-120.

Peters, K. E., Walters, C. C., & Moldowan, J. M. (2007). *The biomarker guide: Volume 1, Biomarkers and isotopes in the environment and human history*. Cambridge university press.

Sendjaja, Y. A., Isnaniawardhani, V., Mursito, A. T., Ramli, T., Mukti, M. M., & Fakhruddin, R. (2024). Geochemistry of Totogan Formation as a potential source rock and its relationship with oil seepage manifestations in the Banjarnegara areas, Central Java, Indonesia. *Heliyon*, *10*(21).

Spacapan, J. B., Palma, J. O., Galland, O., Manceda, R., Rocha, E., D'odorico, A., & Leanza, H. A. (2018). Thermal impact of igneous sill-complexes on organic-rich formations and implications for petroleum systems: A case study in the northern Neuquén Basin, Argentina. *Marine and Petroleum Geology*, *91*, 519-531.

Shen, J., Xie, S., & Xu, Y. (2026). Volcanic effects on the formation of hydrocarbon source rocks. *Science China Earth Sciences*, 1-10.

Svensen, H., Planke, S., Malthe-Sørenssen, A., Jamtveit, B., Myklebust, R., Rasmussen, E., Neumann, E.-R. (2004). Release of methane from a carbonaceous shale during emplacement of a basaltic sill in the Karoo Basin, South Africa. *Earth and Planetary Science Letters*, 217(1-2), 145-157.

Tissot, B.P., Welte, D.H. (1984). *Petroleum Formation and Occurrence*. Springer-Verlag.

Volkman, J. K. (2005). Lipid markers for marine organic matter. In *Marine organic matter: biomarkers, isotopes and DNA* (pp. 27-70). Berlin, Heidelberg: Springer Berlin Heidelberg.

Yandoka, B. M. S., Abdullah, W. H., Abubakar, M. B., Hakimi, M. H., Jauro, A., & Adegoke, A. K. (2016). Organic geochemical characterisation of shallow marine Cretaceous formations from Yola Sub-basin, Northern Benue Trough, NE Nigeria. *Journal of African Earth Sciences*, *117*, 235-251

Yandoka, B. M. S., Abdullah, W. H., Abubakar, M. B., Adegoke, A. K., Maigari, A. S., Haruna, A. I., & Yaro, U. Y. (2017). Hydrocarbon potential of Early Cretaceous lacustrine sediments from Bima Formation, Yola Sub-basin, Northern Benue Trough, NE Nigeria: insight from organic geochemistry and petrology. *Journal of African Earth Sciences*, *129*, 153-164.

Yenne, E., Green, C., & Torvela, T. (2025). Modelling geologic features and structures in the Middle and Lower Benue Trough of Nigeria from gravity and aeromagnetic data sets. *Journal of African Earth Sciences*, *231*, 105745.

Zaborski, P. M., 2003. Guide to the Cretaceous System in the Upper Part of the Upper Benue Trough, Northeastern Nigeria, African Geosciences Review, 10, 13-32.

Zhang, Y., Song, X., & Hou, Z. (2026). Characteristics of Magmatic Intrusions and the Influence on Coal Seams in the Chaigou Coalmine, Datong Coalfield. *Minerals*, *16*(4), 394.